

# FLIGHT DYNAMICS AND CONTROL OF A V-TAIL CAMAR UAV

Mohamad Ashraf Bin Ab Han, Shuhaimi Bin Mansor\*, Mohd Nazri Bin Mohd Nasir

School of Mechanical Engineering, Faculty of Engineering  
Universiti Teknologi Malaysia  
81310 UTM Johor Bahru, Johor, Malaysia

## Article history

Received  
9 September 2020  
Received in revised form  
9 December 2020  
Accepted  
9 December 2020  
Published  
15 December 2020

\*Corresponding author  
shuhaimi@utm.my

## ABSTRACT

The flying qualities for CAMAR-3 UAV needs to be quantified and a control system should be designed with the aspect of longitudinal and lateral static stability, such that CAMAR-3 is responded to efficiently. Therefore, to evaluate the CAMAR-3 efficiency and performance need to be followed by the significance of the analysis of aerodynamic stability coefficients and derivatives. Evaluation of flying qualities of open-loop transfer function can be made through the state-space matrix method. Flight control system have been designed in order to increase the stability of CAMAR-3 UAV in term of longitudinal and lateral stability. The process in designing the control system included the approach of classical control theory, where it was focused on applying simple rate feedback to the system in order to increase the stability. Two different ways have been used to determine the PID parameters, where the PID controller acted as the amplifier gain. The classical control theory has been compared with the modern control theory, where the full state feedback or pole placement method was used to enhance the characteristics of the responses, at the same

time increase the stability. To conclude, modern control design is more suitable for pitch and yaw angle system, while classical control design is more acceptable for roll angle system. For further studies, some recommendations have been made for improvement of CAMAR-3 UAV, including run flight testing of CAMAR UAV to evaluate the aircraft stability after application of the flight control system. Variation of design approach for flight control system can also be used to improve and enhance the aircraft stability.

## KEYWORDS

Flying qualities; state-space; flight control system; rate feedback; PID controller; pole placement.

## INTRODUCTION

Unmanned aerial vehicles (UAV) can be described as one of the classes of aircraft which does not need any pilot on board. Consisting of the aircraft equipment, sensor payloads and a ground control station, the UAV or

also known as a drone can be controlled by using control equipment from the ground. This is a perfect example of Remotely Piloted Vehicle (RPV) where it can be remotely controlled from the ground and involve reliable wireless communication for control.

There are a few factors that can classify the UAV such as the range of altitude, endurance and weight including the wide range applications for military and commercial. For a small and compact size category of UAV, it often comes with the ground-control stations consisting of controller, laptop computers and other components that are small and easy to carry anywhere. Nowadays, UAVs have been fixed with a high precision camera so that it can carry out extra tasks related to navigation and structural analysis. Despite the small size, it is obviously more challenging to operate in turbulence. This can be a massive problem as it can restrain the aircraft from conducting these types of missions. Hence, designing the flight control systems can avoid these problems as most of these systems use classical Proportional-integral-derivative (PID) controllers to tune the controller gains in flight [1].

UAV can also contribute to the aerial exploration capabilities, where it can serve as a platform for communication access points enabling the ad-hoc ground connectivity in areas of lack communication coverage. This issue can be caused by the areas are too remote leading to poor networking infrastructure. A V-tail is described as an unconventional arrangement of the tail control surfaces, which replaces the typical T-tail (fin and horizontal surfaces). These two surfaces set in a V- shaped configuration can be observed from the front or rear of the aircraft. V-tail is designed to reduce the wetted area of the tail and also the weight of the tail [2]. Known as ruddervator, the aft edge of each identical surface is a hinged control surface which carries out both functions of rudder and elevators.

It is essential for every aircraft to achieve the effectiveness of the response to pilot commands in performing flight or mission task element (MTE). The flying and handling qualities are those properties that control the ease and precision of commands given by pilot to the aircraft so it can work accordingly as governed.

A big achievement for UTM researchers as they successfully came out with their Unmanned Aerial Vehicles (UAV) called CAMAR as shown in Figure 1. The CAMAR-1 is the earliest design with comprehensive data from simulation and wind tunnel testing, while the latest CAMAR-3 was developed through Computational Fluid Dynamics (CFD). In relation to the case of study, the flying qualities need to be quantified for CAMAR-3 UAV. To ensure that CAMAR-3 respond efficiently, a controller needs to be designed by taking the aspect of longitudinal and lateral static stability. Thus, the significance of acquiring the aerodynamic stability coefficients and derivatives in order to analyse the performance and stability of CAMAR-3.

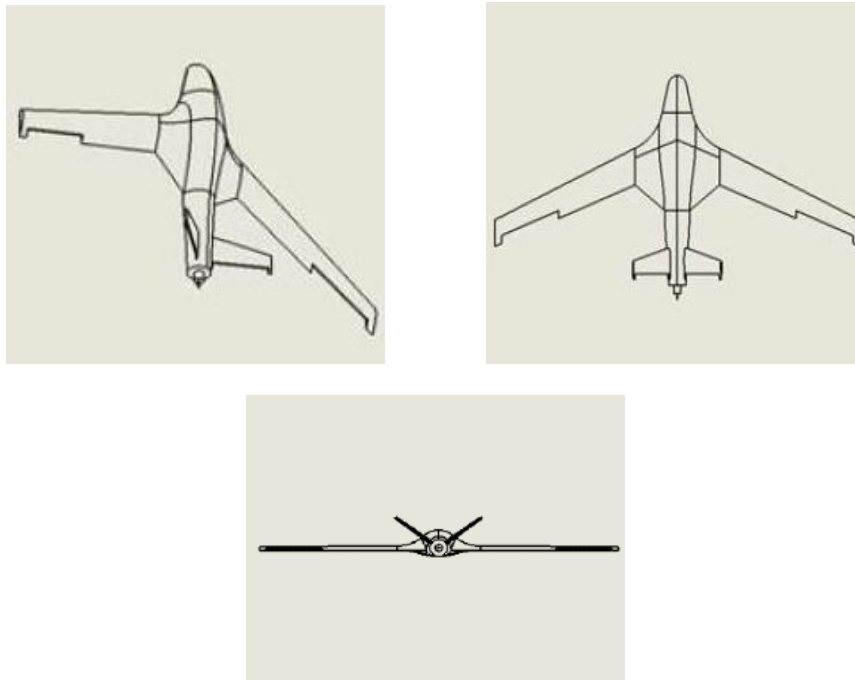


**Figure 1** V-tail CAMAR UAV drawing in Solidworks [3]

## METHODOLOGY

### 1.1 V-Tail CAMAR UAV Specification

The CAMAR UAV with a wingspan of 2.5 meters has a substantial commercialization value for both the local and international market, including mostly are from the defence industries and also local authorities considering the highly experienced operating unmanned system. It involves the defence system against infiltration by foreign forces, pirates and smuggling activities through the provision of surveillance and identification service. With the latest version of CAMAR UAV which is having a configuration of blended wing, it possesses a higher aspect ratio compared to the previous version. The parameter and specification are shown in Figure 2 and Table 1.

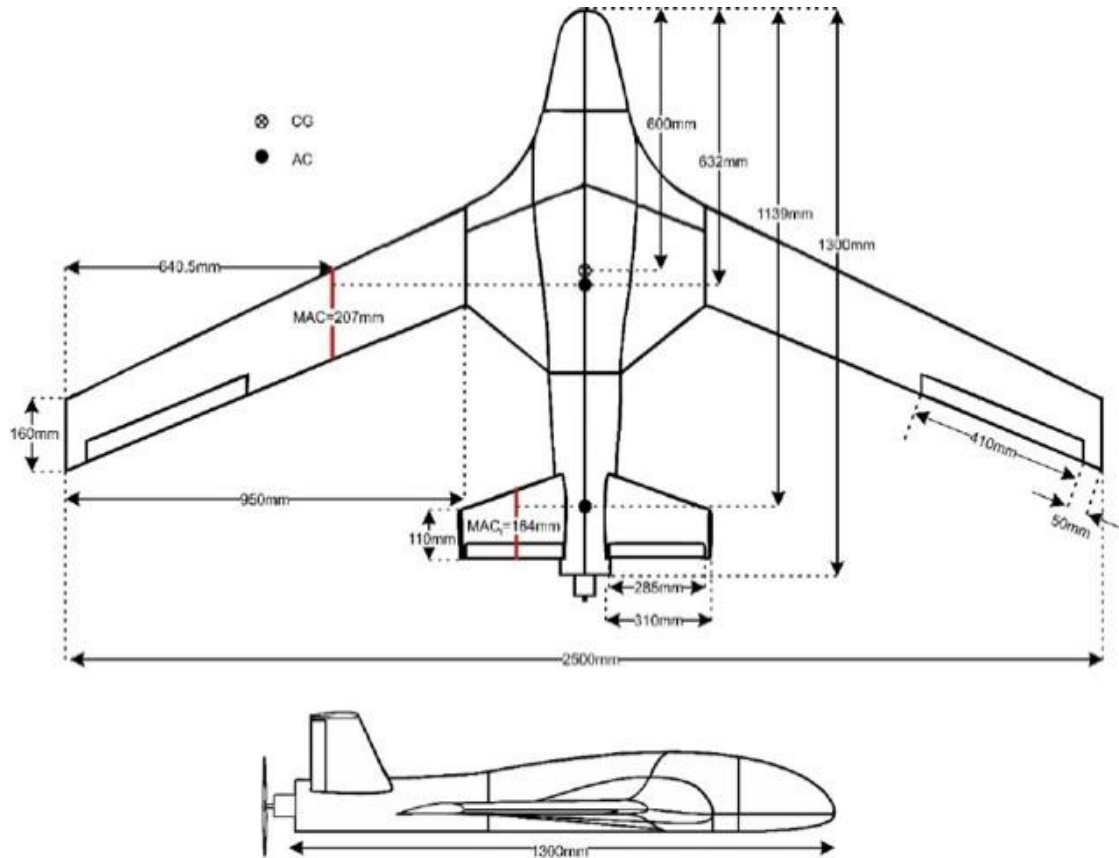


Figure 2 Detailed drawing of V-tail CAMARUAV [3]

Table 1 CAMAR UAV specification

| Specification                   | Symbol    | Value |
|---------------------------------|-----------|-------|
| Maximum Take-Off Weight (kg)    | $m$       | 5     |
| Wing span (m)                   | $b_w$     | 2.5   |
| Wing area ( $m^2$ )             | $S_w$     | 0.51  |
| Wing mean aerodynamic chord (m) | $c$       | 0.207 |
| Wing sweep angle ( $^\circ$ )   | $\Lambda$ | 20    |
| Tail span (m)                   | $b_t$     | 0.62  |
| Tail area ( $m^2$ )             | $S_t$     | 0.151 |
| Tail arm (m)                    | $l_t$     | 0.507 |

|                          |       |       |
|--------------------------|-------|-------|
| CG from nose (m)         | h     | 0.6   |
| Aspect ratio             | AR    | 12.25 |
| Tail volume              | $V_t$ | 0.772 |
| Oswald efficiency factor | $e_f$ | 0.768 |
| Induced drag factor      | k     | 0.034 |

## 1.2 Dimensionless and Dimensional Derivatives

The conventional calculation of the stability derivative is first determining the dimensionless derivatives, followed by the transformation of dimensionless derivatives into the dimensional derivatives which related to their relations [4]. The USAF Stability and Control Data Compendium (DATCOM) is the complete data set for empirical determination of derivatives for subsonic aircraft. This method of determination has been used in J. Roskam, Methods for Estimating Stability and Control Derivatives of Conventional Subsonic Airplanes.

In this section, simple methods can be developed to calculate the aerodynamic stability and control coefficients. Most of the emphasis will be on methods that can be derived from primary theoretical considerations [5]. Such techniques are mostly accurate and show the relationship between the stability coefficients and the geometric and aerodynamic characteristics of the aircraft. In addition, the methods are commonly valid for the subsonic flight only. Nevertheless, the value of derivatives obtained needs to be compared with existing aircraft derivatives to ensure there are no erroneous results.

## 1.3 State-Space Modelling

In the state-space approach, it uses a unique vector-matrix formulation to formulate a dynamic system so it can determine the forced response of typically multiple-input and multiple-output (MIMO) systems. Apart from that, with the same formulation and approach, it can also model the single-input and single-output (SISO) system [6].

Mathematical models of MIMO systems with multiple numbers of outputs result in the same multiple numbers of difference equations, making it hard for the unknown outputs to be determined. Hence, with the state-space approach, the multiple equations can be solved simultaneously by written easily in the state-space form. This application of state variable techniques to control problems can be called as the modern control theory. The reduced differential equations in the previous section can be written in an appropriate matrix form:

$$\dot{x} = Ax + B\eta \quad (1)$$

While for the system output, it is expressed in terms of the state and control inputs:

$$y = Cx + D\eta \quad (2)$$

In this study, by rewriting the linearized longitudinal and lateral equations in the state-space form yields

$$\begin{bmatrix} \Delta \dot{u} \\ \Delta \dot{w} \\ \Delta \dot{q} \\ \Delta \dot{\theta} \end{bmatrix} = \begin{bmatrix} X_u & X_w & 0 & -g \\ Z_u & Z_w & u_o & 0 \\ M_u + M_{\dot{w}}Z_u & M_w + M_{\dot{w}}Z_w & M_q + M_{\dot{w}}u_o & 0 \\ 0 & 0 & 1 & 0 \end{bmatrix} \begin{bmatrix} \Delta u \\ \Delta w \\ \Delta q \\ \Delta \theta \end{bmatrix} + \begin{bmatrix} X_{\delta} & X_{\delta_T} \\ Z_{\delta} & Z_{\delta_T} \\ M_{\delta} + M_{\dot{w}}Z_{\delta} & M_{\delta_T} + M_{\dot{w}}Z_{\delta_T} \\ 0 & 0 \end{bmatrix} \begin{bmatrix} \Delta \delta \\ \Delta \delta_T \end{bmatrix} \quad (3)$$

$$\begin{bmatrix} \Delta\dot{\beta} \\ \Delta\dot{p} \\ \Delta\dot{r} \\ \Delta\dot{\phi} \end{bmatrix} = \begin{bmatrix} Y_{\beta} & Y_p & -\left(1 - \frac{Y_r}{u_o}\right) & g \cos \theta_o \\ u_o & u_o & u_o & \\ L_{\beta} & L_p & L_r & 0 \\ N_{\beta} & N_p & N_r & 0 \\ 0 & 1 & 0 & 0 \end{bmatrix} \begin{bmatrix} \Delta\beta \\ \Delta p \\ \Delta r \\ \Delta\phi \end{bmatrix} + \begin{bmatrix} 0 & Y_{\delta_r} \\ L_{\delta_a} & L_{\delta_r} \\ N_{\delta_a} & N_{\delta_r} \\ 0 & 0 \end{bmatrix} \begin{bmatrix} \Delta\delta_a \\ \Delta\delta_r \end{bmatrix} \quad (4)$$

### 1.4 Flight Control Design

To design a pitch control system, a complete longitudinal flight control system needs to be developed first. This includes the application of rate feedback gain in Stability Augmentation System (SAS) and Control Augmentation System (CAS). An aircraft's stability augmentation system is designed to enhance the aircraft's dynamic characteristics in general [7]. For certain critical flight conditions, for instance, flying in bad weather, the improvement can often be crucial as well. Control augmentation system will be implemented as it can increase the flying qualities up to good Level 1 flying qualities.

By referring to Figure 3, one way to improve the damping ratio on a system is by providing rate feedback,  $k_{rg}$ . This system is known as a pitch rate damper. The artificial damping was provided by the stability augmentation system without interfering with the control input of the pilot. This is achieved by creating an elevator deflection in relation to the pitch rate and applying it to the pilot's control input.

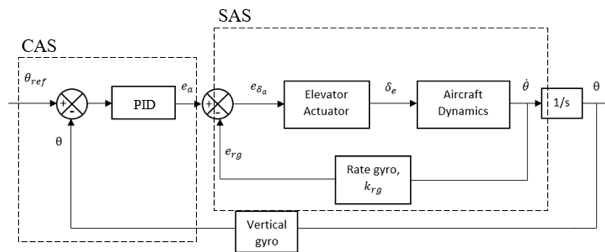


Figure 3 Pitch angle controller block diagram

A servo actuator is needed to make up the control system by developing a transfer function for other elements. It is to deflect the aerodynamic control surfaces and the transfer function for any sensors containing in the control loop. In order to achieve Level 1 of flying qualities, each value of PID gain and  $k_{rg}$  need to be tuned. The method of root locus can be used to obtain both parameters. This is because by obtaining a suitable value of gain, it can increase the stability of V-tail CAMAR UAV. For classical control theory, PID has been used as a controller to read a sensor, then measure the required output of the actuator by measuring the proportional, integral and derivative responses and combine the three parameters to determine the output. It can be written in the form of mathematical equations as:

$$u(t) = K_p e(t) + K_i \int_0^t e(t') dt' + K_d \frac{de(t)}{dt} \quad (5)$$

The purpose of a PID controller is to add the characteristics of proportional, integral and derivative controller types so that a system or process (such as flaps) responds to disturbances or changes in the set-point as required or desired [8]. For this study, the main focus is on making the fine tuning of the proportional (P), proportional integrative (PI), and proportional integrative derivative (PID) control for this project. There are two methods that have been used to determine the PID parameters, which are Ziegler-Nichols method and manual tuning. Meanwhile for modern control theory, pole placement method has been used to design the control system for a better stability. In terms of transient and steady state characteristics, the primary objective in the design of the state-feedback control is to achieve a desirable closed loop response. Full state feedback or pole placement is the method used to put the closed-loop poles of the system in predetermined positions for the design of state feedback controllers. Poles are located corresponds as the eigenvalues of the system, which influences the system's characteristics.

## RESULTS AND DISCUSSION

### 1.5 Stability Dimensionless and Dimensional Derivatives

There are some assumptions been made throughout the calculation of estimation the dimensionless derivatives as the consideration of a low-speed flight condition. Any terms related to the Machnumber can be ignored; for example,  $\partial C_m/M$  and  $C_{D_u}$ . The calculation has been conducted under trimmed flight condition of  $u_0 = 12.8$  m/s and  $\alpha = 7.802^\circ$ .

**Table 2** Coefficients and derivatives for longitudinal stability

| X-force derivatives                         | Z-force derivatives                               | Pitching moment derivatives                       |
|---|---|---|
| $C_{X_u} = -0.0020 \text{ rad}^{-1}$        | $C_{Z_u} = -0.8006 \text{ rad}^{-1}$              | $C_{M_u} = 0 \text{ rad}^{-1}$                    |
| $C_{X_\alpha} = -0.1296 \text{ rad}^{-1}$   | $C_{Z_\alpha} = -5.2910 \text{ rad}^{-1}$         | $C_{M_\alpha} = -2.2120 \text{ rad}^{-1}$         |
| $C_{X_{\dot{\alpha}}} = 0 \text{ rad}^{-1}$ | $C_{Z_{\dot{\alpha}}} = -1.1437 \text{ rad}^{-1}$ | $C_{M_{\dot{\alpha}}} = -2.8013 \text{ rad}^{-1}$ |
| $C_{X_q} = 0 \text{ rad}^{-1}$              | $C_{Z_q} = -4.7354 \text{ rad}^{-1}$              | $C_{M_q} = -11.5983 \text{ rad}^{-1}$             |
| $C_{X_{\alpha_e}} = 0 \text{ rad}^{-1}$     | $C_{Z_{\delta_e}} = -0.2900 \text{ rad}^{-1}$     | $C_{M_{\delta_e}} = -0.7103 \text{ rad}^{-1}$     |
| $X_u = -0.0016 \text{ s}^{-1}$              | $Z_u = -0.6403 \text{ s}^{-1}$                    | $M_u = 0 \text{ (ms)}^{-1}$                       |
| $X_\alpha = -1.3263 \text{ m/s}^2$          | $Z_\alpha = -54.1582 \text{ m/s}^2$               | $M_\alpha = -24.9301 \text{ s}^{-2}$              |
| $X_w = -2.5622 \text{ s}^{-1}$              | $Z_{\dot{\alpha}} = -0.0947 \text{ m/s}$          | $M_{\dot{\alpha}} = 0.0199 \text{ s}^{-1}$        |
| -   | $Z_q = -0.3919 \text{ m/s}$                       | $M_q = -1.0570 \text{ s}^{-1}$                    |
| -   | $Z_{\delta_e} = 2.9685 \text{ m/s}^2$             | $M_{\delta_e} = -8.0055 \text{ s}^{-2}$           |
| -   | $Z_w = -4.2303 \text{ s}^{-1}$                    | $M_w = -1.9477 \text{ (ms)}^{-1}$                 |
| -   | -   | $M_{\dot{w}} = -0.0199 \text{ m}^{-1}$            |

**Table 3** Coefficients and derivatives for lateral stability

| Y-force derivatives                     | Yawing moment derivatives                  | Rolling moment derivatives               |
|---|--|--|
| $C_{y\beta} = -0.208 \text{ rad}^{-1}$  | $C_{n\beta} = 0.028 \text{ rad}^{-1}$      | $C_{l\beta} = -0.001 \text{ rad}^{-1}$   |
| $C_{yp} = 0.426 \text{ rad}^{-1}$       | $C_{np} = -0.143 \text{ rad}^{-1}$         | $C_{lp} = -0.822 \text{ rad}^{-1}$       |
| $C_{yr} = 0.0843 \text{ rad}^{-1}$      | $C_{nr} = -0.0136 \text{ rad}^{-1}$        | $C_{lr} = 0.2897 \text{ rad}^{-1}$       |
| $C_{y\delta_a} = 0 \text{ rad}^{-1}$    | $C_{n\delta_a} = -0.0058 \text{ rad}^{-1}$ | $C_{l\delta_a} = 0.145 \text{ rad}^{-1}$ |
| $C_{y\delta_r} = 0.05 \text{ rad}^{-1}$ | $C_{n\delta_r} = -0.0101 \text{ rad}^{-1}$ | $C_{l\delta_r} = 0.003 \text{ rad}^{-1}$ |
| $Y_\beta = -2.1291 \text{ m/s}^2$       | $N_\beta = 7.0246 \text{ s}^{-2}$          | $L_\beta = -0.2843 \text{ s}^{-2}$       |
| $Y_p = 0.4258 \text{ m/s}$              | $N_p = -3.9706 \text{ s}^{-1}$             | $L_p = -22.8242 \text{ s}^{-1}$          |
| $Y_r = 0.0843 \text{ m/s}$              | $N_r = -0.3776 \text{ s}^{-1}$             | $L_r = 8.0440 \text{ s}^{-1}$            |
| $Y_{\delta_a} = 0 \text{ m/s}^2$        | $N_{\delta_a} = -1.4551 \text{ s}^{-2}$    | $L_{\delta_a} = 41.2279 \text{ s}^{-2}$  |
| $Y_{\delta_r} = 0.5118 \text{ m/s}^2$   | $N_{\delta_r} = -2.5339 \text{ s}^{-2}$    | $L_{\delta_r} = 0.8530 \text{ s}^{-2}$   |

The derivatives are then written in the form of state-space matrix for longitudinal dynamics, yields

$$\begin{bmatrix} \Delta \dot{u} \\ \Delta \dot{w} \\ \Delta \dot{q} \\ \Delta \dot{\theta} \end{bmatrix} = \begin{bmatrix} -0.0016 & -2.5622 & 0 & -9.8100 \\ -0.6403 & -4.2303 & 12.8000 & 0 \\ 0.0128 & -1.8633 & -1.3123 & 0 \\ 0 & 0 & 1 & 0 \end{bmatrix} \begin{bmatrix} \Delta u \\ \Delta w \\ \Delta q \\ \Delta \theta \end{bmatrix} + \begin{bmatrix} 0 \\ 2.9685 \\ -8.0647 \\ 0 \end{bmatrix} [\Delta \delta_e] \tag{6}$$

Where the transfer functions are

$$\frac{\Delta u}{\Delta \delta_e} = \frac{-7.606s^2 + 333.6s + 388.9}{s^4 + 5.544s^3 + 27.77s^2 - 1.562s + 12.23}$$

$$\frac{\Delta w}{\Delta \delta_e} = \frac{2.969s^3 - 99.33s^2 - 0.1589s - 50.28}{s^4 + 5.544s^3 + 27.77s^2 - 1.562s + 12.23}$$

$$\frac{\Delta q}{\Delta \delta_e} = \frac{-8.065s^3 - 39.66s^2 + 13.07s}{s^4 + 5.544s^3 + 27.77s^2 - 1.562s + 12.23}$$

$$\frac{\Delta \theta}{\Delta \delta_e} = \frac{-8.065s^2 - 39.66s + 13.07}{s^4 + 5.544s^3 + 27.77s^2 - 1.562s + 12.23}$$

While for lateral dynamics, the state-space matrix written as

$$\begin{bmatrix} \Delta \dot{\beta} \\ \Delta \dot{p} \\ \Delta \dot{r} \\ \Delta \dot{\phi} \end{bmatrix} = \begin{bmatrix} -0.1663 & 0.0333 & -0.9934 & 0.7660 \\ -0.2843 & -22.8242 & 8.0440 & 0 \\ 7.0246 & -3.9706 & -0.3776 & 0 \\ 0 & 1 & 0 & 0 \end{bmatrix} \begin{bmatrix} \Delta \beta \\ \Delta p \\ \Delta r \\ \Delta \phi \end{bmatrix} + \begin{bmatrix} 0 & 0.0400 \\ 41.2279 & 0.8530 \\ -1.4551 & -2.5339 \\ 0 & 0 \end{bmatrix} \begin{bmatrix} \Delta \delta_a \\ \Delta \delta_r \end{bmatrix}$$

Where the transfer functions can be divided into two, due to rudder input  $\delta_r$  and aileron input  $\delta_a$

$$\frac{\Delta \beta}{\Delta \delta_r} = \frac{0.04s^3 + 3.473s^2 + 62.43s - 15.37}{s^4 + 23.37s^3 + 51.41s^2 + 165.5s - 43.2}$$

$$\frac{\Delta p}{\Delta \delta_r} = \frac{0.853s^3 - 19.93s^2 + 4.155s}{s^4 + 23.37s^3 + 51.41s^2 + 165.5s - 43.2}$$

$$\frac{\Delta r}{\Delta \delta_r} = \frac{-2.534s^3 - 61.36s^2 - 3.552s + 4.038}{s^4 + 23.37s^3 + 51.41s^2 + 165.5s - 43.2}$$

$$\frac{\Delta \phi}{\Delta \delta_r} = \frac{0.853s^2 - 19.93s + 4.155}{s^4 + 23.37s^3 + 51.41s^2 + 165.5s - 43.2}$$

$$\frac{\Delta \beta}{\Delta \delta_a} = \frac{2.817s^2 + 227.3s + 2.96}{s^4 + 23.37s^3 + 51.41s^2 + 165.5s - 43.2}$$

$$\frac{\Delta p}{\Delta \delta_a} = \frac{41.23s^3 + 10.72s^2 + 287.9s}{s^4 + 23.37s^3 + 51.41s^2 + 165.5s - 43.2}$$

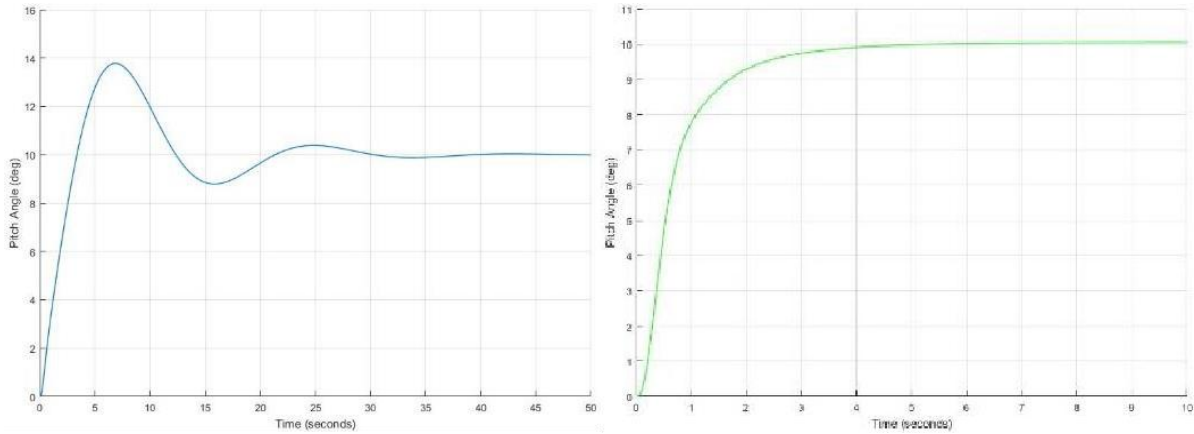
$$\frac{\Delta r}{\Delta \delta_a} = \frac{-1.455s^3 - 197.2s^2 - 23.13s + 221.5}{s^4 + 23.37s^3 + 51.41s^2 + 165.5s - 43.2}$$

$$\frac{\Delta \phi}{\Delta \delta_a} = \frac{41.23s^2 + 10.72s + 287.9}{s^4 + 23.37s^3 + 51.41s^2 + 165.5s - 43.2}$$

## 1.6 Flight Control System

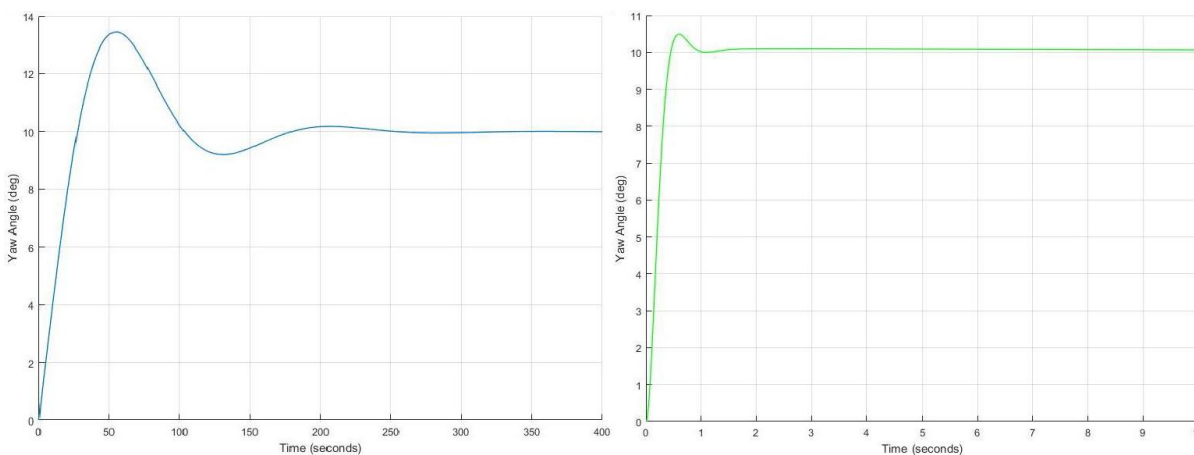
The flight control system was designed for three flight dynamics, which are pitch, yaw and roll. The aim of this study is to create a control system with a good Level 1 flying qualities. To achieve that with response behaviour

of  $\zeta > 0.7$ , value of gain  $k_q$  needs to be approximately decided from the variation of gain value. In this case, the value of  $k_q=0.3$  was taken to satisfy the desired good Level1 handling qualities; eigen values at  $s=-5.17\pm 4.16i$  with correspondence to damping ratio  $\zeta=0.779$  and natural frequency  $\omega_n= 6.63\text{rad/s}$ . After that, further step is to focus on the CAS outerloop design. The Ziegler-Nichols continuous cycling method has been used to determine the PID parameters by referring to the root locus of open loop system pitch rate.



**a) Ziegler-Nichols (b) manualtuning**  
**Figure 4:** Pitch angle response for step input 10 degrees

From Figure 4(a), the trend for Ziegler-Nichols method behaves quite badly, which the rise time reach up to 2.89 seconds, settling time 28.26 seconds and amount of overshoot with 39.36%. Hence, the manual tuning technique was used to tune back the PID parameters under constraints of specifications. The PID parameters obtained from the previous Ziegler-Nichols method were taken as reference to be tuned back by using manual tuning technique. By increasing the gain  $k_p$ , it caused the closed loop system to react more quickly but also to overshoot more. It also tends to reduce the steady - state error of the system. The anticipation of  $k_d$  tends to add damping to the system, which results in decreasing the overshoot. The addition of  $k_i$  will help reducing the steady-state error. The new enhanced value of PID parameters obtained by using the manual tuning technique are  $k_p=1.799$ ,  $k_i=0.01$  and  $k_d= 0.2801$  and the response was plotted in Figure 4(b). With the new optimization, the designed control system now satisfies the requirements; rise time 1.762 seconds, settling time only took 3.171 seconds and amount of overshoot with 0.27%. The same steps were repeated for yaw attitude control system, while amplifier gain was used to replace PID controller for roll angle control system.



**(a) Ziegler-Nichols (b) manualtuning**  
**Figure 5:** Yaw angle response for step input 10 degrees



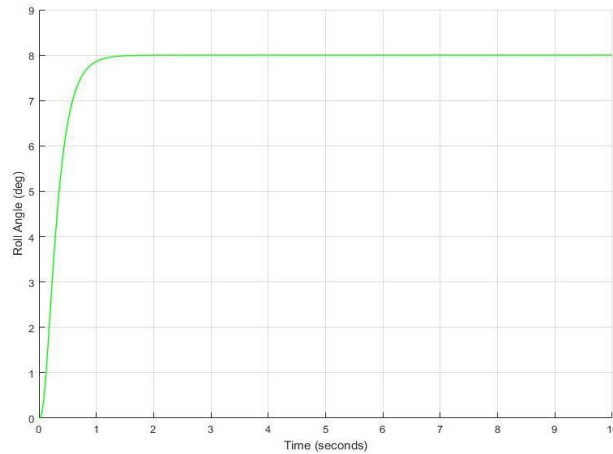
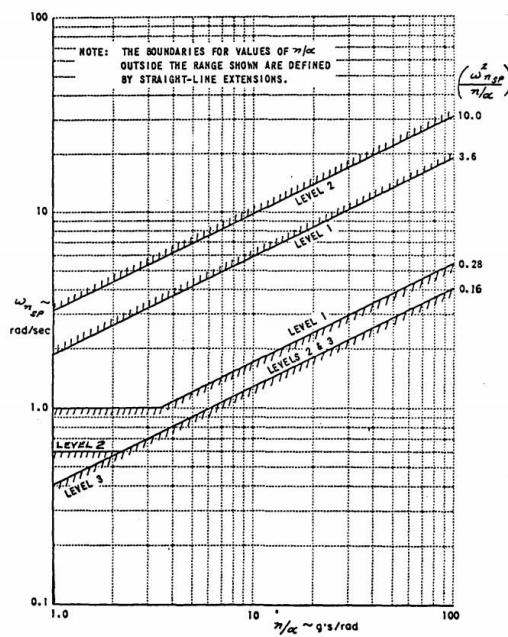


Figure 6: Roll angle response for step input 8 degrees

For modern control theory approach, the state feedback is used to provide a stability augmentation system to improve the CAMAR UAV’s longitudinal and lateral flying qualities. Pole placement is a method applied in feedback control system theory to place the closed-loop poles of a plant in pre-determined locations in the s-plane. This is because the location of the poles corresponds to the eigenvalues of the system, which gives effects to the characteristics of the system response [9]. To improve the stability characteristics of aircrafts that having lack of good flying qualities, state feedback control can be used to change the eigen values of a system. The line aralgebra ice quations were developed in term of unknown feedback gains. MIL-F-8785C short period flying qualities criterion [10] has been taken into consideration in determining the specific requirements in order to obtain Level 1 Control Anticipation Parameter (CAP).



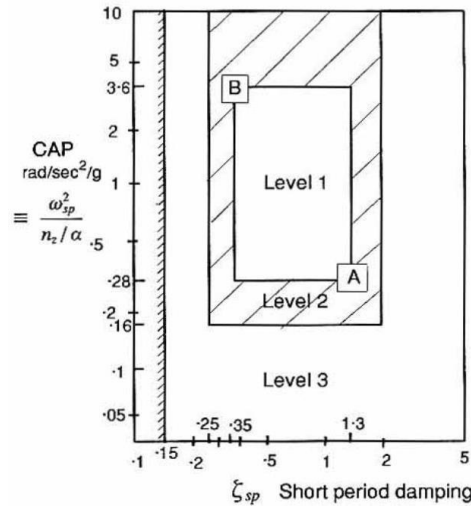
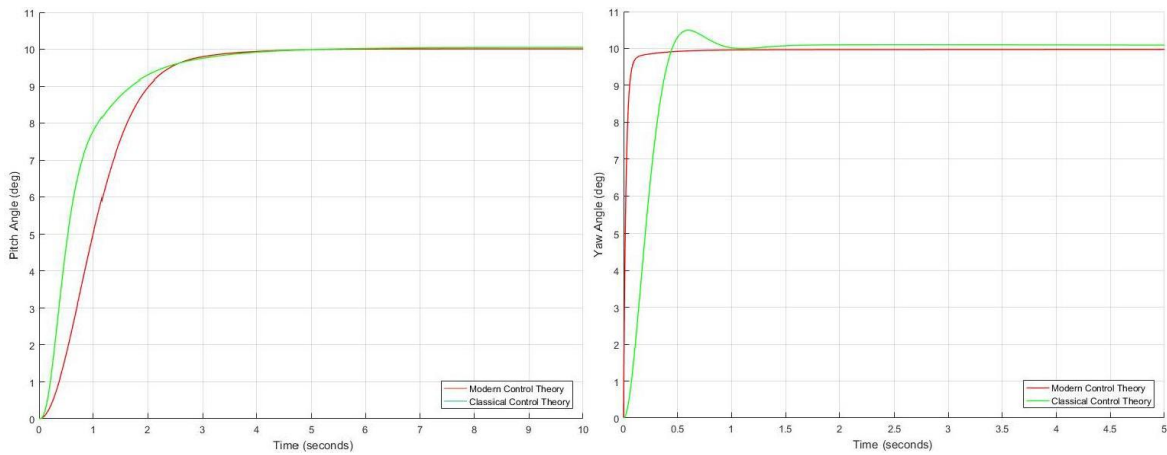
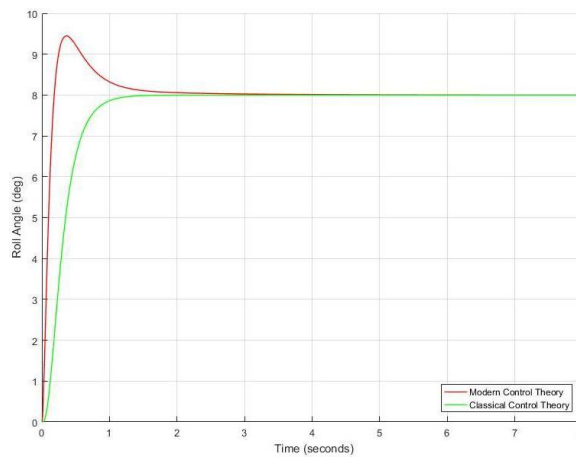


Figure 7: MIL-F-8785C short period flying qualities criterion and CAP against short period damping

For pitch angle, it shows that modern control theory has a better response with rise time 1.649 seconds, settling time 3.051 seconds and overshoot of 0%. The outcomes bring the same result for yaw angle control system where modern control has a better response compared to classical. However, classical control theory gives a better stability in designing roll angle control system as it has a settling time of 0.971 seconds with 0% overshoot.



(a) Pitch angle responses (a) Yaw angle responses



(c) Roll angle responses

Figure 8: Comparison of responses between classical and modern control theory

## CONCLUSION

This project was successful as the value of V-tail CAMAR UAV derivatives can be obtained by conducting semi-empirical method. These derivatives definitely contributed to the results in creating the control system. With the guidance of USAF Stability and Control Data Compendium (DATCOM), this complete empirical analysis set is important for the determination of subsonic aircraft derivatives. By using the state-space approach, multiple equations can be resolved simultaneously, followed by the outcome of respective transfer function. Evaluation of flying qualities of open-loop system are very crucial as it shows that whether the aircraft are stable without the need of any human or machine input. From the evaluation of the open-loop, the flying qualities can be determined and indirectly, a flight control system can be applied to the aircraft to enhance its stability. This includes the application of Stability Augmentation System, Control Augmentation System, Servo Actuator, simple rate feedback and PID. An initiative has been taken by using modern control theory to design the control system as well, including full state feedback (FSF) or pole placement method. Both responses have been compared to decide a better controller.

## ACKNOWLEDGEMENTS

The authors would like to gratefully acknowledge to Prof. Ir. Dr. Shuhaimi Bin Mansor for reviewing and correcting this technical paper.

## REFERENCES

- [1] S. Mansor, Y. Nogoud, S. Mat, M. N. Dahalan, and A. Abdul-latif, "Superaugmented pitching motion of UTM CAMAR UAV using advanced flying handling qualities," *J. Adv. Res. Fluid Mech. Therm. Sci.*, vol. 40, no. 1, pp. 27–37, 2017.
- [2] P. H. Babu, R. Arthurs S.A, S. M. Basha, and S. P, "Design and Analysis of V-Tail Unmanned Air Vehicle (UAV) for Surveillance Application," *Int. J. Eng. Trends Technol.*, vol. 32, no. 3, pp. 119–123, 2016, doi: 10.14445/22315381/ijett-v32p221.
- [3] T. Rashid, "LONGITUDINAL STABILITY OF TAILLESS UAV."
- [4] B. Etkin and L. Reid Duff, "Dynamics of Flight: Stability and Control; Third Edition," *J. Guid. Control. Dyn.*, vol. 20, no. 4, pp. 839–840, 1997, doi: 10.2514/2.4126.
- [5] D. R. C. Nelson, *Flight Stability and Automatic Control*. 2000.
- [6] N. Lobontiu, *System Dynamics for Engineering Students*. .
- [7] S. D. Jenie and A. Budiyo, "Automatic Flight Control System: Classical Approach and Modern Control Perspective," 2006.
- [8] E. C. Alvarez, J. Valentin, and J. Holguino, "Applying Classical Control Theory to an Airplane Flap Model on Real Physical Hardware."
- [9] Y.-Y. Wang, S.-J. Shi, and Z.-J. Zhang, "Pole placement and compensator design of generalized systems," *Syst. Control Lett.*, vol. 8, no. 3, pp. 205–209, 1987, doi: 10.1016/0167-6911(87)90028-4.
- [10] D. O. DEFENSE, "FLYING QUALITIES OF PILOTED AIRCRAFT," *Mil-Std-1797a*, 2004.